Electric quadrupole strength in ^{16}O from the $^{15}N(\vec{p},\gamma_0)^{16}O$ reaction

S. W. Wissink* and S. S. Hanna
Department of Physics, Stanford University, Stanford, California 94305

D. G. Mavis† and T. R. Wang‡
Department of Physics, University of Wisconsin, Madison, Wisconsin 53706

(Received 25 June 1987)

Angular distributions of the relative cross sections and analyzing powers have been measured for the $^{15}N(\vec{p},\gamma_0)^{16}O$ reaction in ≈ 500 keV steps for excitation energies in ^{16}O between 17.8 and 24.9 MeV. All $E1$ and $E2$ transition matrix elements were determined using a partial-wave analysis. Below 22 MeV, little quadrupole strength was found in excess of that predicted in direct capture calculations. A clear enhancement of the $E2$ cross section was observed at energies above 22 MeV. Our data indicate that about 10% of the isoscalar $E2$ sum rule for ^{16}O is exhausted in the p_0 decay channel between 18 and 25 MeV, with approximately $\frac{3}{4}$ of this integrated strength concentrated between 22 and 25 MeV. The $E2$ strength seen in (γ,p_0) is strikingly different from that observed in (α,α') or $(\alpha,\alpha'p)$. The effect of the $M1$ state at $E_x = 18.8$ MeV previously found in (p,γ) studies is clearly observed.

I. INTRODUCTION

It is now well established that nuclei can be excited into various electromagnetic modes of oscillation, classified by their multipolarity: $E1$, $M1$, $E2$, and so on. These excitations, strong and highly collective in nature, are fundamental modes of nuclear motion, observable as resonances in a wide variety of reactions. Though the isovector giant dipole resonance (GDR) has been studied extensively in photonuclear and radiative capture reactions, most information to date on the electric quadrupole ($E2$) strength in medium to heavy nuclei has been obtained through inelastic hadron scattering measurements. These studies show the $E2$ strength to be concentrated within a fairly narrow band of excitation energies, typically 3–5 MeV, and to exhaust a large fraction of the $E2$ sum rule.[1] In lighter nuclei, however, the $E2$ strength appears more fragmented and comparatively weak, providing less definitive evidence for the existence of a compact giant quadrupole resonance (GQR).

For ^{16}O, inelastic α-scattering studies[2] suggest that $\approx 67\%$ of the $(T=0)$ $E2$ energy-weighted sum rule (EWSR) strength lies between 15.9 and 27.0 MeV. Later investigations[3] of the coincident $^{16}O(\alpha,\alpha',c)$ reaction $(c = p_0, p_1, \ldots, \alpha_0, \alpha_1, \ldots,)$ showed the p_0 decay branch to be small and nonresonant between 18 and 27 MeV, exhausting only 9% of the isoscalar EWSR, while significant structure and somewhat more strength (13%) was observed in the α_0 decay channel. These latter results are qualitatively consistent with those seen in the inverse $^{12}C(\alpha,\gamma_0)^{16}O$ studies,[4] though the integrated strength deduced in the inelastic work is twice as large as that seen in radiative α capture. The $^{16}O(\alpha,\alpha'p_0)^{16}O$ results, however, differ markedly from previous studies of the inverse $^{15}N(\vec{p},\gamma_0)^{16}O$ reaction at Stanford[5] and Seattle.[6] These searches for $E2$ strength are in qualitative agreement with each other and suggest that 20–30% of the $(T=0)$ sum rule strength lies between 15 and 30 MeV. Approximately half of this strength is concentrated between 23 and 27 MeV, much higher in excitation energy than in the hadron results.

Other reactions have yielded rather ambiguous information on the integrated strength and energy distribution of the GQR in ^{16}O. In the work of Hotta *et al.*[7] the $E2$ strength seen via electroexcitation between 20 and 30 MeV represents at most 20% of the isoscalar $E2$ sum rule, and no estimate could be made of the strength distribution. The $E2$ strength in the (γ,n_0) or (n,γ_0) channel is comparable[8] to that found in (p,γ_0) measurements. Photoneutron studies at higher excitation energies[9] (30–50 MeV) appear to correlate well with proton capture work[10] and offer evidence for non-$E1$ contributions to the cross section, but a multipole decomposition has not been possible in a model-independent manner. $E2$ strength distributions in ^{16}O have also been obtained by combining elastic photon scattering results with photoabsorption measurements.[11] These data suggest that $1.25^{+1.3}_{-0.9}$ of the total sum rule (isoscalar plus isovector) is exhausted between 22 and 42 MeV, with a distribution at low energy suggestive of that seen in the (p,γ_0) work.

Theoretical descriptions of the GQR and its decay modes are not yet quantitative for the lighter mass nuclei. Early 1p-1h shell model calculations[12–14] could predict the positions of the dominant $E2$ states, but provided little or no information on their widths. Calculations that included a coupling of the nucleons to the continuum[15–17] gave single-particle escape widths much smaller than those experimentally measured ($\Gamma \approx 1$ MeV in ^{16}O), suggesting that the major contribution to the observed width comes from the spreading width, i.e., the coupling of the 1p-1h states to more complex configurations. These ideas have been developed rigorously in several theoretical calculations,[18–20] and in each case strong fragmentation of the giant $E2$ state was found. In the

work of Dehesa *et al.*,[20] three strong isoscalar $E2$ states are predicted to lie between 16 and 26 MeV, exhausting 55% of the $T=0$ sum rule.

In summary, our knowledge of the $E2$ strength in ^{16}O remains rather unclear and often contradictory. There are significant differences between the proton capture and alpha capture results, and both of these differ from the hadron scattering work. In an attempt to resolve some of the existing experimental discrepancies, we have reexamined with higher precision the $^{15}N(\vec{p},\gamma_0)^{16}O$ reaction ($Q=12.126$ MeV), measuring the angular distributions of the emitted photons, and taking advantage of the powerful analysis techniques this procedure allows for sufficiently simple spin sequences. By extracting the amplitudes and phases of all $E1$ and $E2$ transition matrix elements, we have determined the distribution of the $E2$ strength as a function of excitation energy in ^{16}O, as observed in the proton ground state decay channel.

II. EXPERIMENTAL TECHNIQUE

The photon yields from the reaction $^{15}Ne(\vec{p},\gamma_0)^{16}O$ were measured at nine detector angles between 25° and 155° for incident proton bombarding energies between 6.25 and 13.75 MeV, stepped in 500 keV intervals. The experiment was conducted with the model EN tandem Van de Graaff accelerator at the University of Wisconsin–Madison Nuclear Physics Laboratory. The intense polarized beam ($\approx$300–400 nA) used was provided by the Wisconsin colliding-beam polarized negative ion source.[21] Proton polarizations were typically 88–91 % and stable to better than 1% over long periods.

The target gas cell consisted of a vertical cylindrical steel chamber 3.81 cm in diameter. A slot in this chamber subtending an angle of 245° and covered with a nickel foil 1.9 μm thick, served not only as the entrance and exit foil for the beam, but also as a thin window for all outgoing photons of interest. To suppress background, the gas cell, the back wall of the scattering chamber, and the entire beam dump were lined with clean lead sheets. The target was N_2 gas enriched to $\approx$99% in ^{15}N. The cell pressure was monitored to approximately $\pm$0.02%, relatively. The pressure averaged 400 mm Hg, corresponding to an effective target thickness of 2.7 mg/cm^2.

Prior to each run, the center of the scattering chamber was aligned with the center of rotation of the NaI crystal assembly. Mylar targets were used to generate exact images of the beam profile, 2.2 mm in diameter. A transit indicated less than a 0.25 mm discrepancy between beam center and the true center of rotation. Use of a double slit system, with current feedback to steerers, kept the beam centered both horizontally and vertically during data acquisition.

The capture γ rays were detected in a single cylindrical crystal of NaI(Tl), 25 cm long by 25 cm in diameter. The crystal is viewed by six low gain phototubes matched to high count rate bases. Energy resolution is typically 2.2% for 22 MeV γ rays at low counting rates, with a free-running gain stability of better than 1% per day. The use of transistor-stabilized bases kept gain shifts to less than 0.2% for detector rates up to 400 kHz.

The crystal is surrounded by an annulus of plastic scintillator (NE102) 10 cm thick, segmented into six identical optically insulated pieces, each viewed by two phototubes. This annulus serves to tag those events in which either the full energy of the photon is not deposited within the NaI crystal, or which are generated by stray sources of radiation, such as cosmic rays or the beam dump. Low energy background components are greatly attenuated by jackets of lead and of $^6Li_2CO_3$, as was done previously.[22]

The complete assembly is mounted on a carriage which can rotate about the target spot and allows for varying the distance from target to detector. The detector collimator was designated to just illuminate the entire back face of the NaI crystal at a distance of 62 cm from target to the front of the collimator. At this distance, the detector subtended a solid angle of 35 msr and could be rotated from 23° to 156°.

Three solid-state charged particle detectors were mounted inside the target chamber directly above, below, and to the right of the gas cell, which allowed the beam position (both vertical and horizontal), relative beam polarization, and target thickness to be monitored continuously. All three detectors were double-slit collimated to ensure that only particles scattered from the target gas could reach the detectors.

Absolute measurements of the proton polarization were made with a standard ^4He polarimeter[23–25] mounted 5 m downstream from the main scattering chamber. The polarization state of the incident beam was reversed every 2.5 s during both the polarization measurements and actual data acquisition.

The electronics used for signal processing and routing is fairly standard.[26,27] After the six NaI phototube outputs are fast summed, passive filter shaping is used to decrease the long signal decay times. A high-level discriminator used in conjunction with a fast low-level updating discriminator serves to reject a severe low energy background produced largely through thermal and fast neutron capture.

For the anticoincidence annular shield, the two phototube outputs from each plastic segment are first added, then independently amplified and fast summed. The segmented configuration of the plastic annulus allows for faster, more uniform light collection, and the plastic-NaI coincident resolving time was typically 8 ns. This combination of fast pileup rejection and nanosecond timing results in an energy resolution of better than 3% for a 22 MeV photon at detector rates up to 400 kHz, and gives less than a 10% accidental rejection of valid events for count rates in the annulus up to 4 MHz.

All NaI signals that exceeded the high level discriminator and satisfied the no pileup requirement were routed to either an accept or reject spectrum, the latter consisting of those events in which a coincident signal was detected in the plastic shield. A branch of slow shaping electronics improved the spectrometer resolution by processing only valid events. An externally triggered tail pulse was also fed into the NaI fast-summing box, and appeared as a narrow "high energy" peak in the spectra. Typical

spectrometer performance is illustrated by Fig. 1 in which most of the features mentioned above can be observed.

At each bombarding energy, at least two complete angular distributions were measured, the angles being swept in opposite directions. The proton polarization was measured immediately before and after each scan. At the end of each scan, an on-line analysis program performed simple γ-ray and particle monitor peak sums, retrieved necessary scaler information, and then calculated all yields and correction factors due to pulse pileup losses, electronic dead time, and accidental rejection of valid events by the anticoincidence shield. The program also ensured that all gain shifts and most electronic or detector malfunctions would be immediately noted. The first-pass analysis served only to monitor on-line the integrity of the data.

III. DATA REDUCTION

To determine the number of counts in the γ_0 peaks (Fig. 1), the 18 spectra accumulated during a given scan were first summed, after adjusting the energy scale at each angle to correct for center-of-mass effects. In the summed spectrum, the peak region (whose limits were defined to be certain fractions of the centroid) was then fit with a third-order spline curve constrained at the end points to approach physically acceptable asymptotic values. This procedure provided an analytic expression for a line shape that could then be used to fit each of the individual peaks from the same scan, varying only the peak centroids and amplitudes from angle to angle.

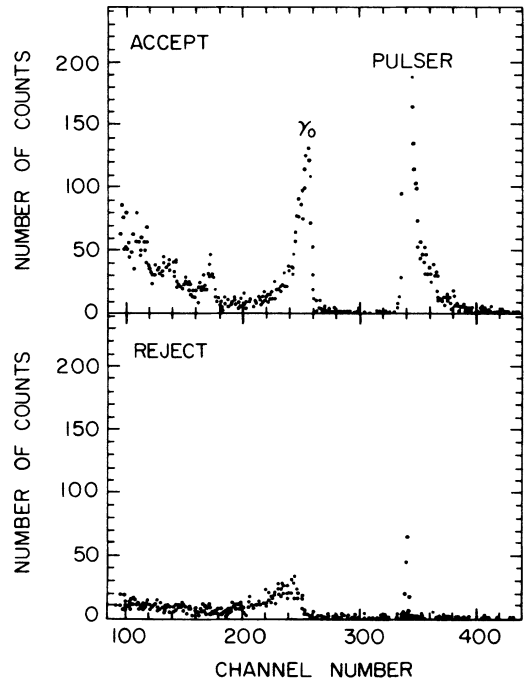

FIG. 1. The accept and reject spectra obtained with spin-up protons at $E_p = 10.64$ MeV for $\theta_\gamma = 90°$. The γ_0 and pulser peaks are visible near channels 254 ($E_\gamma = 22.08$ MeV) and 340 (peak off scale), respectively. In this figure zero energy is at -128 channels.

The integrated areas under the fitted line shapes were converted into relative γ-ray yields as follows. To correct for rate-dependent losses, the peak areas from the Accept spectra were multiplied by the ratio of the number of pulser counts generated to the number of pulser events that actually appeared in the accept spectrum. This factor accounts for losses due to pileup rejection, accidental anticoincidence veto, and any analog-to-digital converter (ADC) dead time; typical values were 15%, 1–2%, and 0.2%, respectively. Because the NaI counting rate was held constant for all angles, the pileup rejection rate was essentially angle independent.

The accidental anticoincidence rejection rate was determined by comparing pulser peak areas in the accept and reject spectra after a flat background, due largely to cosmic rays, was subtracted from the latter. The values obtained for the accidental rejection rates were found to scale very closely with the observed counting rates in the plastic annulus.

Normalization of the measured γ_0 yields to either the integrated beam current or to the particle monitor yields produced no statistically significant differences, and the particle monitor results were used throughout. Center-of-mass conversions were also made before the yields from the various scans were combined into a final set of angular distributions.

The differential cross section for a radiative capture reaction initiated by a polarized proton can be separated into its polarization-dependent and -independent components by writing it in the form

$$\sigma_\gamma(E_p,\theta_\gamma;\mathbf{P}_p)=\sigma_0(E_p,\theta_\gamma)[1+\mathbf{P}_p\cdot\mathbf{n}\,A(E_p,\theta_\gamma)]\ , \tag{1}$$

where $\sigma_0(E_p,\theta_\gamma)$ is the usual unpolarized cross section, $A(E_p,\theta_\gamma)$ is the vector analyzing power for the reaction, $\mathbf{P}_p$ is the incident proton polarization, and $\mathbf{n}$ is a unit vector defined by the Madison convention to lie along $\mathbf{k}_{in}\times\mathbf{k}_{out}$.

The functions σ_0 and A can be written as series expansions of the rotation matrices. For the differential cross section σ_0, summing over all possible spin states for all particles collapses the expression into a simple sum of Legendre polynomials[28]

$$\sigma_0(E,\theta)=\sum_{k=0}^{k_{max}} A_k(E)P_k(\theta)$$

$$=A_0(E)\left[1+\sum_{k=1}^{k_{max}} a_k(E)P_k(\theta)\right]\ , \tag{2}$$

where unnecessary subscripts have been dropped. Similarly, the polarization-dependent term involves a summation over all spins except that of the incident proton, and reduces to a sum of associated Legendre polynomials,[28]

$$\sigma_0(E,\theta)A(E,\theta)=\sum_{k=1}^{k_{max}} B_k(E)P_k^1(\theta)$$

$$=A_0(E)\sum_{k=1}^{k_{max}} b_k(E)P_k^1(\theta)\ . \tag{3}$$

In this notation the total cross section is given by

$$\sigma_{\rm tot}(E)=4\pi A_0(E) ,$$

so A_0 carries the information on the resonance strength, while the fractional coefficients $\{a_k=A_k/A_0, b_k=B_k/A_0\}$ completely specify the (normalized) angular distributions. The value of $k_{\rm max}$ is equal to twice the multipolarity of the highest multipole transition considered.[28]

For a given spin and parity configuration, the a_k and b_k coefficients can be expressed in terms of the reduced matrix elements R_t for the various allowed reaction channels t, in the form

$$a_k=\sum_{t,t'} C(t,t',k)\,\mathrm{Re}(R_t,R_{t'}^*) , \tag{4a}$$

$$b_k=\sum_{t,t'} D(t,t',k)\,\mathrm{Im}(R_t,R_{t'}^*) , \tag{4b}$$

where $(R_t,R_{t'}^*)$ represents the product of (complex) channel matrix elements. Explicit expressions for $C(t,t',k)$ and $D(t,t',k)$ have been given by Seyler and Weller[29] and Glavish,[30] and special cases have been tabulated.[31]

For the reaction $^{15}\mathrm{N}(\vec{p},\gamma_0)^{16}\mathrm{O}$, a given multipolarity excitation can occur through just two reaction channels. If $E1$ and $E2$ transitions are the dominant radiations, only $s_{1/2}$ and $d_{3/2}$ capture (to form the $E1$ 1^- states) and $p_{3/2}$ and $f_{5/2}$ capture (for the $E2$ 2^+ states) are allowed. The reaction matrix can then be completely specified in terms of seven independent parameters (four complex matrix elements, with one phase arbitrary). Because $k_{\rm max}=4$ for this case, the photon yield data can be characterized by nine coefficients [see Eqs. (1)–(3)], and the extraction of the complete reaction matrix from the experimental data is overdetermined. The full expressions relating the seven capture amplitudes and phases to the nine experimentally determined angular distribution coefficients are given explicitly in Appendix A. Complications that arise from the inclusion of other multipole radiations, chiefly $M1$, will be discussed herein.

The analysis program used in this investigation fit all normalized γ_0 yields (usually 18) for a given energy simultaneously. In the first phase of the analysis, the nine angular distribution coefficients $(A_0,\ldots,A_4,B_1,\ldots,B_4)$, were determined at each energy by fitting Eqs. (1)–(3) to the data by a standard linear least-squares method. These coefficients were then corrected for the finite solid angle acceptance of the NaI spectrometer,[32] and for linear target effects using an iterative procedure.

The second phase of the analysis involved a least-squares fit, based on the algorithm of Marquardt,[33] of all seven reaction matrix parameters directly to the corrected yields, i.e., one uses Eqs. (1)–(3), but inserts the expressions for the A_k and B_k coefficients given in Appendix A explicitly into the minimization equations. From these quantities one can determine the contribution of each multipolarity to the total radiative capture cross section. This procedure assumes that only $E1$ and $E2$ excitations are present at measurable levels. Nevertheless, the nonlinearity of these expressions often resulted in multiple solutions, and more extensive statistical analysis was frequently warranted.

IV. RESULTS

A. Angular distributions fits

A sample of the unpolarized differential yields and reaction analyzing powers determined in this investigation is shown in Fig. 2. At each energy, the data were normalized against the value of A_0 calculated for each scan, and the results averaged over all scans. The solid lines are the theoretical curves calculated from the best fit

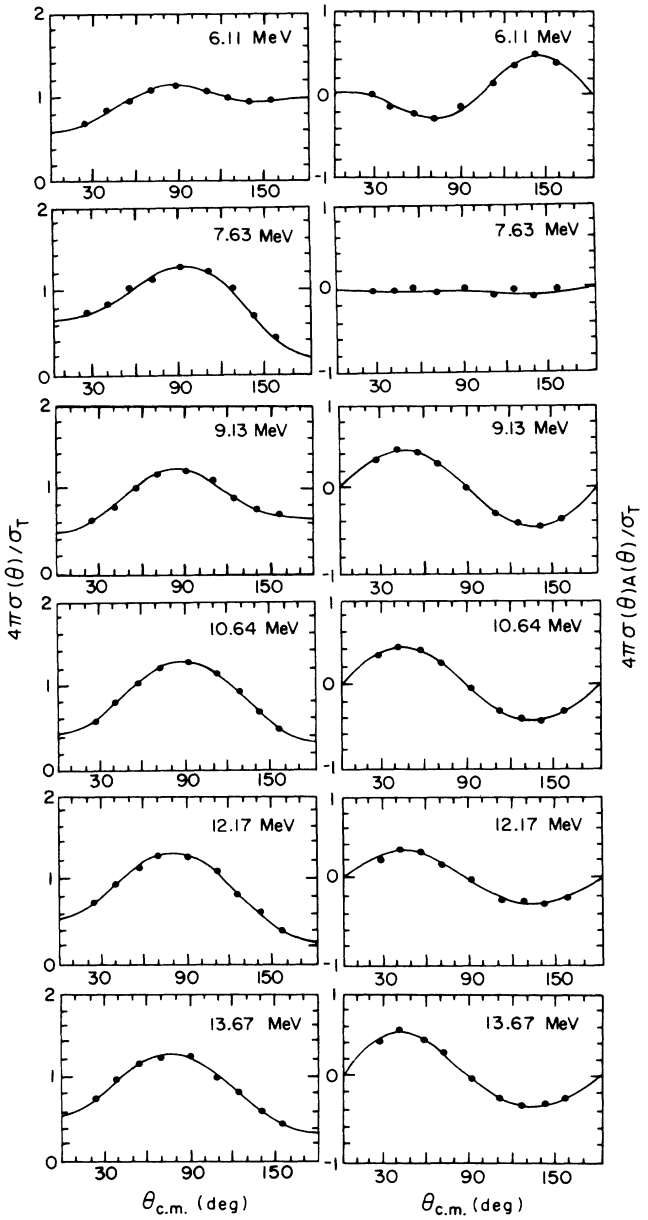

FIG. 2. A sample of the unpolarized differential yields, $\sigma(\theta)$ (normalized to A_0), and the analyzing powers, $\sigma(\theta)A(\theta)$, determined in the $^{15}\mathrm{N}(\vec{p},\gamma_0)^{16}\mathrm{O}$ reaction. The error bars are smaller than the dots. The corresponding proton energy at the center of the target gas cell is provided on each plot. Solid lines are calculated from the fitted values of the a_k and b_k coefficients.

values of the a_k and b_k coefficients.

The predominance of $E1$ radiation is clearly seen, especially at $E_p = 10.64$ MeV, near the peak of the GDR in ^{16}O. The yields and analyzing powers follow closely the $\sin^2\theta$ and $\sin 2\theta$ angular dependences, respectively, predicted for pure electric dipole radiation. Deviations indicate the presence of other multipolarities; in particular, a loss of symmetry (antisymmetry) about 90° in the differential yield (analyzing power) results specifically from interfering radiation of the opposite parity, which suggests $E2$ or $M1$ strength. Though such deviations are most apparent at lower energies, they may be noticeable here only because of the great decrease in absolute $E1$ strength.

The fitted values for the expansion coefficients are shown as functions of excitation energy in Fig. 3. The final values for A_0 deduced in this study are also plotted, after having been scaled to force our value for A_0 at $E_p = 10.64$ MeV to match the cross section measured previously[34] at this energy. This single conversion factor produced very acceptable agreement between the two experiments, lending confidence to the normalization procedures employed to obtain absolute strengths.

In the region of the GDR, roughly 20–25 MeV, the a_2 and b_2 coefficients are large in magnitude and relatively constant. This would suggest that the $E1$ giant resonance is either characterized by a nuclear configuration that changes only slightly with excitation energy, or, as suggested by Mavis,[35] gives rise to similar angular distributions even if the basic configuration changes. Some rather striking fluctuations do occur in these coefficients near 21 and 23 MeV, especially in the a_2 values. These deviations appear to be correlated with structure in the $E1$ total cross section, and may indicate interference between the various dipole states.[36,37]

The nonzero odd a_k and b_k coefficients can be taken as unambiguous evidence for the presence of radiation of positive parity (given that the dominant radiation is indeed $E1$), presumably $E2$, $M1$, or both. The nonzero $k=3$ terms then indicate at least some $E2$ strength at almost all energies. Interpretation of the a_1 and b_1 coefficients is more difficult, since they are sensitive to both $E2$ and $M1$ radiations. We only point out that b_1 is generally fairly close to zero, except for a value of -0.4 measured just below 19 MeV. The significance of this result for possible $M1$ strength will be discussed herein.

The small $k=4$ coefficients support our hypothesis that the $E2$ strength is weak relative to $E1$ radiation, and that contributions from even higher multipoles, such as $E3$ radiation, are negligible at these excitation energies. This last possibility was investigated more rigorously by extending some of the fits to include polynomials up through order $k=6$. In all cases, the values obtained for the $k=5$ and 6 coefficients were consistent with zero within statistics, and no significant decreases were seen in the χ^2_ν values for the fits.

As an independent test of these assumptions, one can compare the distribution of χ^2_ν values obtained to the distribution expected theoretically, as shown in Fig. 4 for our 36 fits to the individual scans. The overall agreement seems reasonable for the small sample size considered.

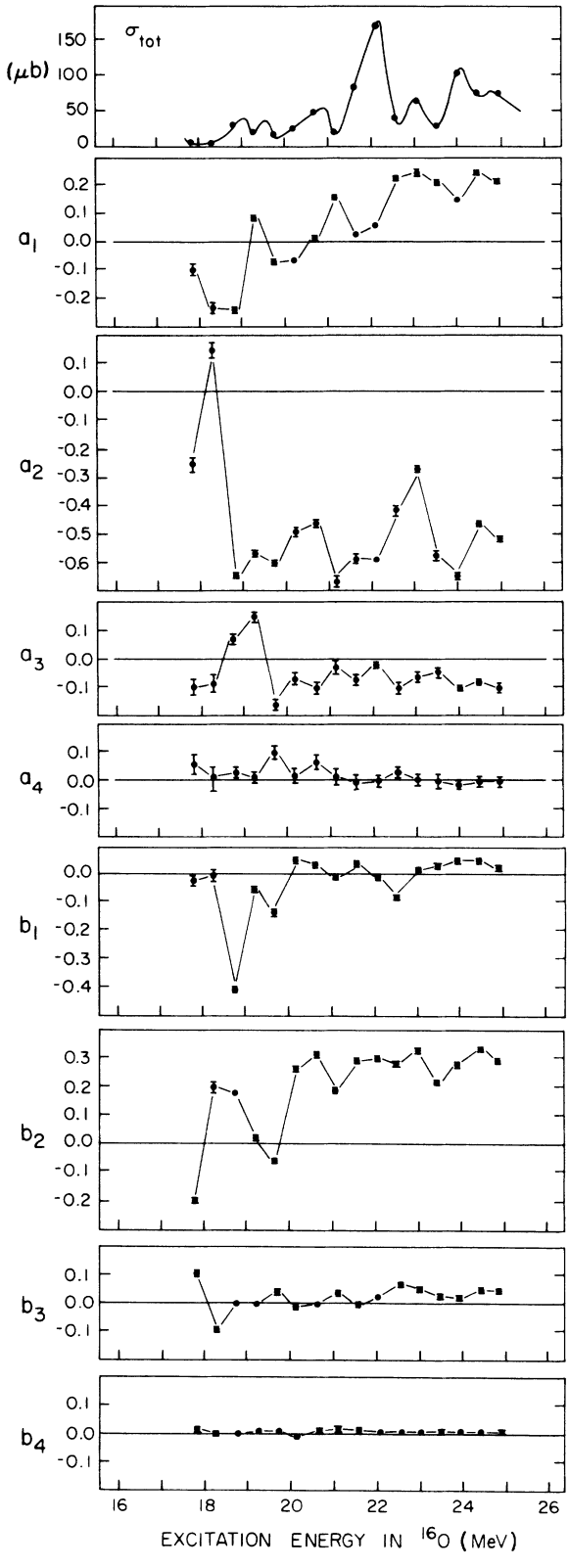

FIG. 3. Final values determined for the Legendre and associated Legendre polynomial expansion coefficients a_k and b_k, respectively, obtained from a fit to order $k=4$. Error bars not visible are smaller than the dots. Renormalized values for $A_0(\sigma_{tot})$ are compared to the total cross section data of O'Connell and Hanna (Ref. 34) and Wissink *et al.* (Ref. 44).

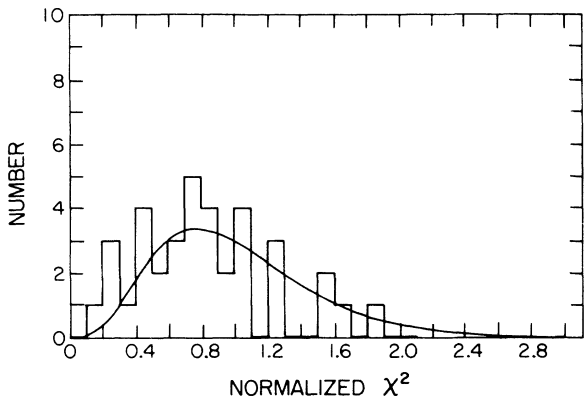

FIG. 4. Distribution of the reduced χ^2_ν values obtained in fits of the Legendre and associated Legendre polynomials to the polarized yields measured in the individual scans. The smooth curve shown is the predicted distribution of fits with nine degrees of freedom for a sample size of 36.

B. Reaction matrix fits

Pure $E1$ radiation will lead to a twofold degeneracy in the values extracted for the various matrix elements, an ambiguity intrinsic to the nature of the defining equations.[5] The reasonable assumption that $E1$ radiation dominates the cross section suggest that a similar degeneracy should still exist. In our searches for $E2$ strength, we used two different sets of starting parameters, one which assumed a dominant s-wave capture solution for the $E1$ matrix elements, the other a dominant d-wave solution. In each case the starting values of the p- and f-wave amplitudes were both taken to be small, typically 5–10%, which corresponds to $E2$ strengths on the order of 1% of the total cross section.

The capture amplitudes extracted through this procedure are shown as functions of excitation energy in Fig. 5 for both the dominant d-wave and dominant s-wave solutions. In most theoretical calculations, the GDR is excited most strongly via an $l \rightarrow l+1$ transition with no spin flip. Because these models predict a dominant $p \rightarrow d$ transition in ^{16}O, we will limit our discussions to the d-wave solution. (The reduced χ^2_ν values and the $E2$ strengths deduced for the two solutions did not differ from each other by more than 0.1% at any energy.)

The $E1$ parameters, shown in the upper portion of Fig. 5, are relatively constant throughout the GDR, from roughly 20 to 25 MeV. The phase difference in this region does not exhibit any strong correlation with the structure seen in the cross section, and no dramatic changes occur in the d-wave to s-wave amplitude ratio as one moves through energy regions where the dipole resonance configuration is predicted to be changing radically.[38]

The partial wave capture amplitudes for $E2$ excitations are shown in the lower part of Fig. 5. The solution corresponding to a dominant d wave shows a p-wave amplitude that is small and relatively featureless; the seemingly larger values below 20 MeV reflect only an overall decrease in $E1$ strength, since we have normalized these

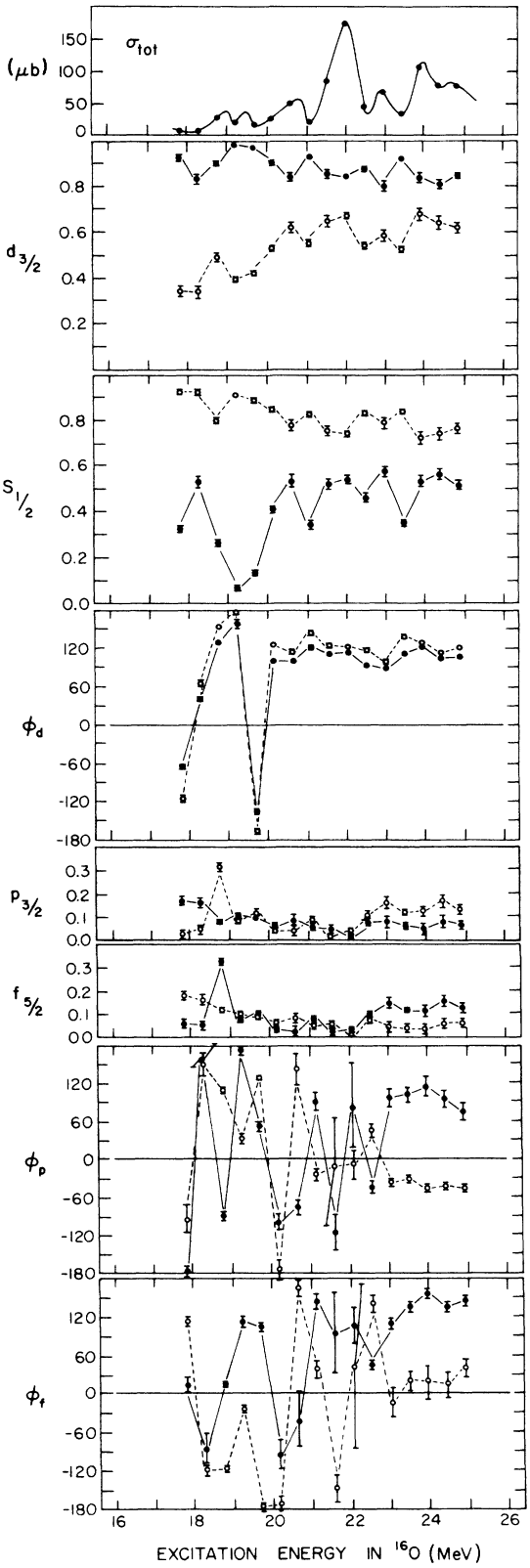

FIG. 5. Final values determined for the normalized $E1$ and $E2$ capture amplitudes and phases. Both dominant d-wave (solid points) and dominant s-wave (open circles) solutions are shown. The total cross section curve is explained in the caption of Fig. 3. The d, p, and f wave phases are taken relative to the s wave phase.

amplitudes against the total capture cross section.

The relative f-wave amplitude is also small, but significantly nonzero, even in regions of fairly large total cross section. The singularly high point seen at 18.8 MeV must not be considered valid because of the poor quality of the fit at this energy. Above 22 MeV there is clear evidence for an increase in the f-wave amplitude. The phases of the $p_{3/2}$ and $f_{5/2}$ matrix elements both show rapid fluctuations at all but the highest energies. The correlations seen between the two phases suggest a relatively constant phase difference between the two $E2$ matrix elements, much like that observed for the $E1$ matrix elements.

The solution corresponding to dominant s-wave capture is also shown for completeness. Most of the general features noted above are reproduced by this set of fitted values, though this choice of $E1$ parameters appears to reverse the "roles" of the $E2$ parameters as well, i.e., the $f_{5/2}$ amplitude is small and devoid of any suggestive structure, while the $p_{3/2}$ amplitude peaks at the higher energies.

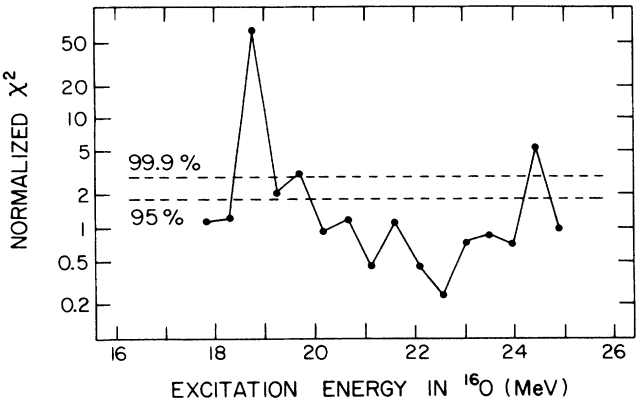

FIG. 6. The reduced χ^2_ν values, obtained in fits of the $E1$ and $E2$ capture amplitudes to the polarized yield data, plotted versus excitation energy in ^{16}O. The two dashed horizontal lines denote the level below which the indicated percentage of all points are expected to lie. To relate these points to the giant resonance structure of ^{16}O, reference can be made to the total cross section curve of Fig. 3.

C. Treatment of $M1$ radiation

To determine absolute $M1$ strengths, additional information is required, either from more complete experiments or from theoretical models. As yet, theoretical predictions are not of sufficient quality to be quantitatively useful, nor have the necessary experiments been performed, e.g., detecting the polarization of the outgoing photon.

One means of searching for possible $M1$ strength is suggested by the equations that relate the angular distribution expansion coefficients to the reaction capture amplitudes. If one neglects the $M1$ parameters (as in the Appendix) during the fitting process, yet these matrix elements are contributing to the measured yields, this deficiency should manifest itself in the values of χ^2_ν that one obtains. Figure 6 shows our minimum χ^2_ν values plotted versus excitation energy.

Note first the cluster of potentially "unacceptable" values around 19 MeV. The quality of the fit at 18.8 MeV is sufficiently poor that the results of our $E1$-$E2$ analysis at this energy must be considered essentially useless, even though analysis in terms of Legendre and associated Legendre polynomials yielded very satisfactory fits (χ^2_ν's of 1.00 and 0.25 for the two scans). The existence of $M1$ strength in this region has also been predicted theoretically[39] and observed in other experiments.[40,41] The situation is somewhat more ambiguous for the two adjacent points between 19 and 20 MeV. Although the χ^2_ν values are down by a factor of more than 20 from the value at 18.8 MeV, these two points remain high. When one considers the narrow width attributed to the 18.8 MeV state (120 keV in Ref. 41), it is not inconceivable that two separate states of non-$E1$ or non-$E2$ character exist in this region.

A more intriguing problem arises near 24.5 MeV, where the χ^2_ν is again very high. For the lower energy points just discussed, the poor χ^2_ν was due almost entirely to the anomalously large negative values found for the b_1 coefficient, which might be attributable to significant ($E1$,$M1$) interference effects. The 24.5 MeV data, however, yielded fairly "typical" values for all the a_k and b_k coefficients, and the deduced $E1$ and $E2$ amplitudes and phases seem quite reasonable compared to those at neighboring energies. On the basis of these arguments, one cannot rule out the possibility of $M1$ strength in this region, but there is little evidence to support this explanation for the poor quality of the fit.

Because $M1$ radiation contributes almost exclusively to the $k=1$ expansion coefficients, one can reduce the sensitivity of the analysis to $M1$ strength by artificially decreasing the statistical weighting given to these coefficients in the analysis. An approach used in previous studies was to eliminate the a_1 and b_1 coefficients entirely, by either excluding them from a fit directly to the coefficients,[5] or by deleting appropriate rows and columns from the full error matrix in a sequential fitting process.[6] Because there are no degrees of freedom left in the fitting procedure, χ^2_ν will vanish identically if a solution is possible, and one cannot test the applicability of the fitting equations used.

In this work, both of the above methods have been used. The $E2$ strengths determined by this technique were consistently larger than those deduced in the fits to all the data by factors of 1.5–5, with error bars enlarged by similar amounts. Attempts to use the capture amplitudes determined without the $k=1$ coefficients to predict a_1 and b_1 also generally resulted in values that were too large, with errors often an order of magnitude greater than those determined in the original fits to the data. At several energies the predicted $k=1$ coefficients differed by more than two standard deviations from those measured, though there was no obvious correlation between these energies and those for which the χ^2_ν values discussed earlier were anomalously large. No clear interpretation of these results was found.

D. Discussion of $E2$ strength

Even if one could be sure that all sources of systematic error had been properly handled, and all effects due to $M1$ radiation were known to be negligible, the nonlinearity of the fitting equations, coupled with low statistics, can often result in ambiguities in extraction of the $E2$ strengths. There are at least two degenerate minima in the χ_ν^2 surface for $E2$ strength, corresponding to the dominant s-wave and dominant d-wave $E1$ solutions. Several additional secondary minima may also exist where searching routines might get trapped, thereby missing the true minimum. To locate as many of these minima as possible, it is useful to constrain the $E2$ strength to some constant value while allowing all other parameters to vary. By minimizing the value of χ_ν^2 for a fixed $E2$ strength, the searching routine is forced to follow certain contours along the χ_ν^2 surface, specifically contours of constant p^2+f^2. Mapping out the projection of this surface onto the $E2$ strength axis not only enhances one's ability to locate multiple minima, but provides important qualitative information on the goodness of the fit.

The $E2$ strength, expressed as a fraction of the total yield, was therefore stepped from 0.0 to 0.2 in increments of 0.01, though the region below 0.05 often required study under finer resolution. The same set of starting parameters was used for all fits so that "continuity" would not push the search vector along valleys in the χ_ν^2 surface, rather than permitting it to step coarsely over the allowed contour. In all cases, a dominant d-wave solution was assumed for the initial values for the parameters.

The results of this analysis are illustrated in Fig. 7 for all of the data. At most energies, the χ_ν^2 curve has a single, relatively sharp minimum. The five highest energies, 23.0–24.9 MeV, demonstrate this type of behavior, even in regions of large $E2$ strength, though the large value of the χ_ν^2 minimum at 24.45 MeV is disturbing. At lower excitation energies a secondary minimum appears more frequently, but usually corresponds to a statistically unacceptable value for χ_ν^2. One exception occurs at 21.6 MeV, where the two minima represent essentially equally good fits. More curious is the 20.7 MeV data, the only case where the minimum corresponding to the higher value of $E2$ strength produced a lower value for χ_ν^2. In the study by Bussoletti[6] a similar pattern was observed at $E_x = 20.4$ MeV, lending credence to these results.

The final regime of interest centers about the three points near 19 MeV noted earlier for their unacceptably high χ_ν^2 values. The 18.8 MeV data yield a single broad minimum, but at a totally unacceptable confidence level. At both 19.3 and 19.7 MeV a second minimum is suggested, but at an unreasonably large $E2$ strength. It is not clear what significance can be ascribed to this behavior, given the possible presence of $M1$ radiation at these energies.

Bearing all of the above in mind, we present in Fig. 8 the final values determined in this work for the $E2$ cross section as a function of excitation energy in ^{16}O. The $E2$ strengths shown are those that correspond to the smallest χ_ν^2 value found at that energy. All $E2$ strengths for secondary minima falling below the 1% confidence level are displayed as well, since these alternate fits cannot be discarded *a priori* as "spurious" solutions; the point at 18.8 MeV, however, has been omitted as being meaningless. Also shown for reference are the results of a direct capture calculation.[42]

Because our primary goal in this work is to map out

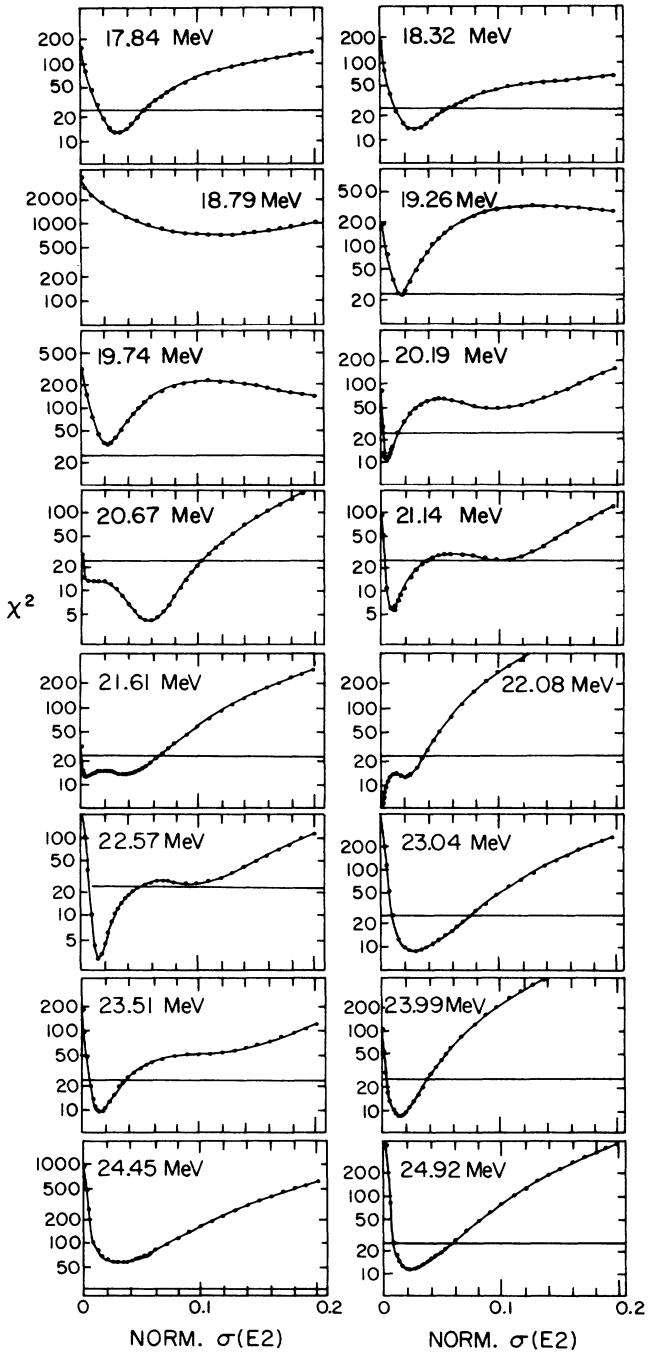

FIG. 7. Curves of χ_ν^2 minima for stepped values of the normalized $E2$ cross sections. The corresponding excitation energy is provided on each plot. The solid horizontal line indicates the 1% confidence level for these functions. Actual fitting results appear as points; the smooth curves are drawn only to guide the eye.

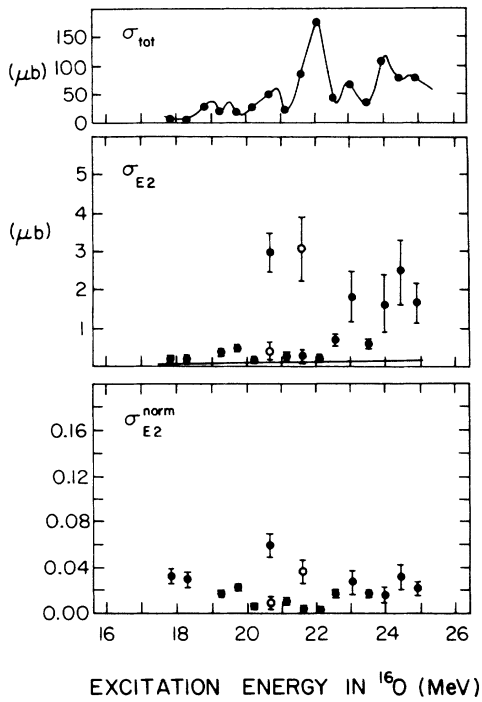

FIG. 8. Final values determined for the absolute and normalized (to σ_{tot}) $E2$ cross sections for the reaction ^{15}N(p,γ_0)^{16}O. Open circles indicate additional solutions falling below the 1% confidence level. The total cross section curve is explained in the caption of Fig. 3. The smooth curve in the σ_{E2} plot is the result of a direct capture calculation (Ref. 42). The datum at 18.8 MeV is omitted because of its unreasonably large value of χ^2_ν (see the text).

the $E2$ strength distribution in a search for resonant behavior, the energies above 22 MeV are of greatest interest. The χ^2_ν curves for these energies were all characterized by a single, well-defined minimum at an acceptable level of statistical confidence, except for the 24.4 MeV point where the minimum occurred at a rather high value of χ^2_ν. The pronounced enhancement in the extracted $E2$ cross sections compared to those obtained at lower energies is obvious, as is the excess of $E2$ strength over that predicted in the direct capture calculation.

To evaluate this increase in strength quantitatively, we compare the integrated observed strength to that of the appropriate sum rule, which is the energy-weighted integral of the total photonuclear cross section over all excitation energies.[1] For isoscalar $E2$ transitions, we have

$$\sum_c \int \frac{\sigma_{E2}(\gamma,c)}{E_x^2} dE_x = (\pi^2\alpha/3M_pc^2)(Z^2/A)\langle r^2\rangle ,$$

where M_p is the proton mass, Z and A are the proton and nucleon numbers of the photonuclear target nucleus, and $\langle r^2\rangle$ is its mean square nuclear charge radius. The sum over c is a reminder that one must include the photonuclear strengths observed in all decay channels. If we use $\langle r^2\rangle^{1/2}=2.72$ fm, as determined by DeJager *et al.*[43] from electron scattering data, the isoscalar $E2$ sum rule value is 7.56 μb/MeV. For the isovector $E2$ sum rule a numerically equivalent result is obtained for self-conjugate nuclei, although meson exchange effects may modify this result.

To compare our integrated $E2$ cross section to the sum rule, the radiative capture results must be converted to the corresponding photonuclear cross sections. Using the principle of detailed balance, one finds

$$(2J_f+1)E_\gamma^2\sigma(\gamma,p_0) = (2J_t+1)(M_t/M_f)^2(2M_pc^2E_p)\sigma(p,\gamma_0) ,$$

where J_x and M_x are the spins and masses for the target ($x=t$) and final ($x=f$) nuclei, M_p is the proton mass, and E_γ and E_p are the lab energies of the incident photon and proton, respectively.

In determining our integrated strength, the $E2$ cross section deduced at 18.8 MeV was replaced by an average of the cross sections at the two adjacent energies. At 20.7 and 21.6 MeV the lower $E2$ values were selected, based largely on continuity arguments. Both of these lower values were obtained in fits with a χ^2_ν less than 1.3, so these solutions are not unreasonable. With these assumptions, we find that 9.8±1.2 % of the isoscalar $E2$ sum rule is exhausted between 17.8 and 24.9 MeV. If the larger $E2$ value is used for either the 20.7 or 21.6 MeV data, this figure increases to 12.4±1.3 % or 12.5±1.4 %, respectively.

If one considers just the energy region between 22.6 and 24.9 MeV, which encompasses the six highest excitation energies studied, one finds an integrated $E2$ strength corresponding to 7.0±1.1 % of the sum rule. Subtracting the calculated direct capture components of the cross section decreases the strength found in this region to 6.1±1.1 %, where the error quoted does not account for possible uncertanties in the results of the direct capture calculations. For energies below approximately 22.5 MeV, there is little $E2$ strength in excess of that attributable to direct capture, unless either one or both of the two higher $E2$ strengths are taken to be the correct value.

Though we have observed a quadrupole resonance near 24 MeV in ^{16}O, the assignment as a "giant" resonance requires that a significant fraction of the appropriate sum rule be exhausted when summed over all decay channels. To make such a comparison, knowledge of the p_0 branching ratio, Γ_{p_0}/Γ, is required. In the coincidence work of Knöpfle *et al.*[3] this quantity is estimated to average about 30% for excitation energies between 24 and 27.3 MeV. If one assumes all the $E2$ strength seen in the present work to be due to isoscalar transitions, this would imply that perhaps 20–25 % of the $E2$ sum rule is exhausted in an energy range of just slightly more than 2 MeV.

V. OTHER WORK

Previous estimates of the $E2$ strength seen in the ^{15}N(p,γ_0)^{16}O reaction tend to be in qualitative agreement with these results. Earlier Stanford studies[5] found a similar enhancement in the extracted $E2$ cross section above 23 MeV, but LaCanna's measurements suggest that 38% of the $E2$ sum rule is exhausted in the somewhat wider

energy range between 22 and 27 MeV. In a study by Bussoletti,[6] the same type of structure was also observed near 24 MeV. Integrating from 19 to 29 MeV, Bussoletti found approximately 28% of the isoscalar $E2$ sum rule, though this was considered to be a lower limit. In a reanalysis of the data by Snover,[6] in which some new lower energy results were included, the integrated $E2$ strength was estimated at 12–22 % of the sum rule between 17.9 and 27.3 MeV.

In Fig. 9 results from the present work are compared with those from hadronic excitation of the $E2$ strength in ^{16}O. In (α,α') excitation,[2] the $E2$ strength is seen to be concentrated in a resonantlike structure between $E_x = 17$ and 26 MeV. It is clear that the $E2$ strength seen in the (γ,p_0) channel (the present work) bears very little resemblance to the (α,α') curve in shape or location. This dissimilarity is heightened by a comparison with the $(\alpha,\alpha'p)$ coincidence results.[8] Although 9% of the isoscalar $E2$ sum rule was found to lie in the proton ground state decay channel when integrated between 18 and 27 MeV,

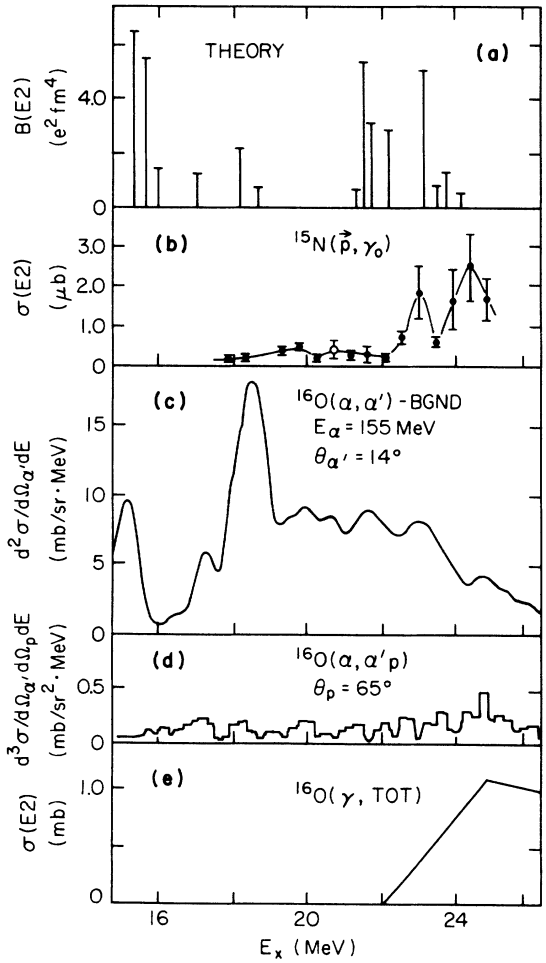

FIG. 9. Comparison of $E2$ strength in this experiment with other work: (a) random-phase approximation calculation based on $1p1h+2p2h$ excitations (Ref. 18); (b) the (p,γ_0) reaction, present data; (c) the inelastic (α,α') excitation (Ref. 2); (d) the $(\alpha,\alpha'p)$ coincidence process for $E_p > 4$ MeV (Ref. 3); and (e) photon scattering experiment (Ref. 11).

which is quite consistent with the results found here, it is disturbing that in the $(\alpha,\alpha'p_0)$ work no resonant effect was observed to correspond with either the (p,γ_0) or (α,α') results. This would suggest that the pronounced enhancement seen above 22 MeV in the present work may be due to the onset of the isovector $E2$ resonance.

A meaningful comparison can be made between the present (γ,p_0) result and the total $E2$ cross section observed in γ scattering and absorption,[11] also shown in Fig. 9. In this case, there is remarkably good agreement in the location of the major $E2$ strength, which in the photon experiment was seen to extend up to 42 MeV, and corresponds to 1.25 times the total isoscalar plus isovector sum rules. The $E2$ strength derived from (γ,n_0) measurements[8] is also in reasonable agreement with the present results.

There have been many calculations of the $E2$ strength in ^{16}O based on variety of models and interactions. At the top of Fig. 9 we show the results of a calculation[18] which incorporates 2p-2h excitations into the basic 1p-1h, $2\hbar\omega$ configurations. We see that the predicted strength is not only spread out widely, in agreement with the various measurements, but there is a strong local concentration of strength in the region where it has been observed in the (p,γ_0) and photon experiments.

Finally, our results at $E_x \approx 18.8$ MeV agree with those of Snover *et al.*[45,40] who postulated the existence of a relatively strong $M1$ level at this energy and estimated some parameters for the state. The existence of this state has also been confirmed in (e,e') (Ref. 41) and (p,p') (Ref. 46) excitations.

VI. SUMMARY AND CONCLUSIONS

In this investigation we have performed precise measurements of the angular distributions of the photons emitted in the decay to the ground state of the ^{16}O nucleus following polarized proton capture by ^{15}N. Knowledge of the reaction yields and analyzing powers allows one to determine all the complex $E1$ and $E2$ capture amplitudes in a model-independent manner, if one assumes these to be the only multipolarities contributing significantly to the (p,γ_0) cross section. Studies were made for incident proton bombarding energies in the range of 6.25–13.75 MeV, which corresponds to excitation energies in ^{16}O between 17.8 and 24.9 MeV. Below 22 MeV, no quadrupole strength was found in excess of that predicted in direct capture calculations, although the data at two energies were somewhat ambiguous. A clear enhancement of the $E2$ cross section was observed at energies above 22 MeV, but it was not possible to make a realistic estimate of the resonance centroid or width. Our data indicate that only 10% of the isoscalar $E2$ sum rule is exhausted in the p_0 decay channel between 18 and 25 MeV excitation energy. Approximately 70% of this integrated strength is concentrated between 22 and 25 MeV.

ACKNOWLEDGMENTS

We are grateful to Professor Claus Rolfs for the direct capture cross section calculations. Two of us (S.W.W.

and S.S.H.) would like to thank Professor Willy Haeberli for the hospitality extended to us during the experiments at Madison. This work was supported by the National Science Foundation.

APPENDIX A: EQUATIONS FOR THE ANGULAR DISTRIBUTION COEFFICIENTS

The expressions relating the angular distribution coefficients of the polarized proton capture differential yield to the actual reaction matrix parameters are unfortunately far from standardized in form. In this work we have adhered as much as possible to the conventions established by Glavish[30] and now codified by Seyler and Weller.[29] The equations used here will differ only by a normalization factor relating the capture amplitudes to the true reduced reaction matrix elements.

We will designate the angular momentum values relevant to a radiative capture reaction in the following way:

$$a(x,L)c \ . \tag{A1}$$

In our notation, a is the spin of the target nucleus, x the (intrinsic) spin of the incident particle, l the orbital angular momentum in the entrance channel, b the spin of the intermediate state excited in the final nucleus, L the multipolarity of the emitted photon, p the electromagnetic mode of the photon (electric=1, magnetic=0), and c the spin of the final nuclear ground state.

We work in the j-j coupling representation, where j is the total angular momentum brought in by the incident particle. The various angular momenta are coupled according to the following scheme:

$$\begin{aligned} &\mathbf{l}+\mathbf{x}=\mathbf{j} \ , \\ &\mathbf{j}+\mathbf{a}=\mathbf{b}=\mathbf{L}+\mathbf{c} \ . \end{aligned} \tag{A2}$$

For the reaction ^{15}N(p,γ_0)^{16}O, $c=0$, so $L=b$. We can therefore unambiguously specify the reduced transition matrix elements by

$$R_{lj}^{pL}=\langle pLc;b\|R\|(lx)ja;b\rangle \ . \tag{A3}$$

The complex capture amplitudes referred to throughout this work are explicitly defined by

$$l_j e^{i\phi_{lj}}=(\lambda/2)\hat{x}^{-1}\hat{a}^{-1}\hat{b}R_{lj}^{pL} \ , \tag{A4}$$

where $\hat{j}\equiv(2j+1)^{-1/2}$, etc. Because of this direct relationship, the expressions "capture amplitudes" and "reaction matrix elements" have been used interchangably.

For brevity, we adopt the notation

$$(s_{1/2},p_{3/2})\equiv\phi_{s_{1/2}}-\phi_{p_{3/2}}, \text{ etc.} \ ,$$

and, for $E1$ and $E2$ radiation from ^{15}N(p,γ_0)^{16}O, we find

$$\begin{aligned}
A_0&=s_{1/2}^2+d_{3/2}^2+p_{3/2}^2+f_{5/2}^2 \ , \\
A_1&=\sqrt{6}s_{1/2}p_{3/2}\cos(s_{1/2},p_{3/2})-(\sqrt{3}/5)d_{3/2}p_{3/2}\cos(d_{3/2},p_{3/2})+9(\sqrt{2}/5)d_{3/2}f_{5/2}\cos(d_{3/2},f_{5/2}) \ , \\
A_2&=\sqrt{2}s_{1/2}d_{3/2}\cos(s_{1/2},d_{3/2})-\tfrac{1}{2}d_{3/2}^2+\tfrac{1}{2}p_{3/2}^2-(\sqrt{6}/7)p_{3/2}f_{5/2}\cos(p_{3/2},f_{5/2})+\tfrac{4}{7}f_{5/2}^2 \ , \\
A_3&=2s_{1/2}f_{5/2}\cos(s_{1/2},f_{5/2})+6(\sqrt{3}/5)d_{3/2}p_{3/2}\cos(d_{3/2},p_{3/2})-4(\sqrt{2}/5)d_{3/2}f_{5/2}\cos(d_{3/2},f_{5/2}) \ , \\
A_4&=8(\sqrt{6}/7)p_{3/2}f_{5/2}\cos(p_{3/2},f_{5/2})-\tfrac{4}{7}f_{5/2}^2 \ , \\
B_1&=(\sqrt{6}/2)s_{1/2}p_{3/2}\sin(s_{1/2},p_{3/2})-2(\sqrt{3}/5)d_{3/2}p_{3/2}\sin(d_{3/2},p_{3/2})-9(\sqrt{2}/10)d_{3/2}f_{5/2}\sin(d_{3/2},f_{5/2}) \ , \\
B_2&=-(\sqrt{2}/2)s_{1/2}d_{3/2}\sin(s_{1/2},d_{3/2})+5(\sqrt{6}/42)p_{3/2}f_{5/2}\sin(p_{3/2},f_{5/2}) \ , \\
B_3&=-\tfrac{2}{3}s_{1/2}f_{5/2}\sin(s_{1/2},f_{5/2})+2(\sqrt{3}/5)d_{3/2}p_{3/2}\sin(d_{3/2},p_{3/2})+(\sqrt{2}/15)d_{3/2}f_{5/2}\sin(d_{3/2},f_{5/2}) \ , \\
B_4&=-2(\sqrt{6}/7)p_{3/2}f_{5/2}\sin(p_{3/2},f_{5/2}) \ .
\end{aligned} \tag{A5}$$

Using the above notation, we can determine the absolute strengths of the contributing multipoles using the equations

$$\sigma_{\text{tot}}=4\pi A_0=\sigma_{E1}+\sigma_{E2} \tag{A6}$$

and

$$\begin{aligned} \sigma_{E1}&=4\pi(s_{1/2}^2+d_{3/2}^2) \ , \\ \sigma_{E2}&=4\pi(p_{3/2}^2+f_{5/2}^2) \ , \end{aligned} \tag{A7}$$

where σ is a total cross section, in units (for example) of μb, or, equivalently, μb/4πsr.

*Present address: Indiana University Cyclotron Facility, Bloomington, IN 47405.
†Present address: Mission Research Corporation, 1720 Randolph Rd. S.E., Albuquerque, NM 87106.
‡Present address: Kellogg Radiation Laboratory, California Institute of Technology, Pasadena, CA 91125.

[1]M. Gell-Mann and V. L. Telegdi, Phys. Rev. **91** 169 (1953).
[2]K. T. Knöpfle, G. J. Wagner, H. Breuer, M. Rogge, and C. Mayer-Böricke, Phys. Rev. Lett. **35**, 779 (1975).
[3]K. T. Knöpfle, G. J. Wagner, P. Paul, H. Breuer, C. Mayer-

Böricke, M. Rogge, and P. Turek, Phys. Lett. **74B**, 191 (1978).
[4]K. A. Snover, E. G. Adelberger, and D. R. Brown, Phys. Rev. Lett. **32**, 1061 (1974).
[5]S. S. Hanna, H. F. Glavish, R. Avida, J. R. Calarco, E. Kuhlmann, and R. LaCanna, Phys. Rev. Lett. **32**, 114 (1974); R. LaCanna, Ph.D. thesis, Stanford University, 1977.
[6]J. E. Bussoletti, Ph.D. thesis, University of Washington, 1978; K. A. Snover, in *Giant Multipole Resonances*, edited by F. E. Bertrand (Harwood Academic, New York, 1980), p. 229.
[7]A. Hotta, K. Itoh, and T. Saito, Phys. Rev. Lett. **33**, 790 (1974).
[8]J. W. Jury, J. S. Hewitt, and K. G. McNeill, Can. J. Phys. **48**, 1635 (1970).
[9]T. W. Philips and R. G. Johnson, Phys. Rev. C **20**, 1689 (1979).
[10]P. Paul, J. W. Noe, K. A. Snover, M. Suffert, E. K. Warburton, and H. M. Kuan, in *Proceedings of the International Symposium on Highly Excited States in Nuclei, Jülich, 1975*, edited by A. Faessler, C. Mayer-Böricke, and P. Turek (Kernforschunsalage, Jüich, 1975), Vol. 1, p. 2.
[11]W. R. Dodge, E. Hayward, R. G. Leicht, M. McCord, and R. Starr, Phys. Rev. C **28**, 8 (1983).
[12]S. Krewald and J. Speth, Phys. Lett. **52B**, 295 (1974).
[13]G. F. Bertsch and S. F. Tsai, Phys. Rep. **18C**, 125 (1975).
[14]K. F. Liu and G. E. Brown, Nucl. Phys. **A265**, 385 (1976).
[15]S. Krewald, J. Berkholz, A. Faessler, and J. Speth, Phys. Rev. Lett. **33**, 1386 (1974).
[16]S. Shlomo and G. Bertsch, Nucl. Phys. **A243**, 507 (1975).
[17]K. F. Liu and N. van Giai, Phys. Lett. **65B**, 23 (1976).
[18]W. Knüpfer and M. G. Huber, Z. Phys. A **276**, 99 (1976).
[19]T. Hoshino and A. Arima, Phys. Rev. Lett. **37**, 266 (1976).
[20]J. S. Dehasa, S. Krewald, J. Speth, and A. Faessler, Phys. Rev. C **15**, 1858 (1977).
[21]W. Haeberli, M. D. Barker, C. A. Gossett, D. G. Mavis, P. A. Quin, J. Sowinski, T. Wise, and H. F. Glavish, Nucl. Instrum. Methods **196**, 319 (1982).
[22]M. Suffert, W. Feldman, J. Mahieux, and S. S. Hanna, Nucl. Instrum. Methods **63**, 1 (1968).
[23]M. D. Barker, P. C. Colby, W. Haeberli, and P. Signell, Phys. Rev. Lett. **48**, 918 (1982).
[24]P. Schwandt, T. B. Clegg, and W. Haeberli, Nucl. Phys. **A163**, 432 (1971).
[25]F. Sperisen, W. Grüebler, V. König, P. A. Schmelzbach, B. Jenny, K. Elsener, C. Schweizer, and J. Ulbricht, Phys. Lett. **102B**, 9 (1981).
[26]S. L. Blatt, J. Mahieux, and D. Kohler, Nucl. Instrum. Methods **60**, 221 (1968).
[27]E. M. Diener, J. F. Amann, S. L. Blatt, and P. Paul, Nucl. Instrum. Methods **83**, 115 (1970).
[28]S. Devons and L. J. B. Goldbarb, in Nuclear Reactions III, Vol. 42 of Hanbuch der Physik, edited By S. Flügge (Springer-Verlag, Berlin, 1957), p. 362.
[29]R. G. Seyler and H. R. Weller, Phys. Rev. C **20**, 453 (1979).
[30]H. F. Glavish, Nuclear Physics Laboratory, Stanford University, Internal Report, 1970 (unpublished).
[31]R. W. Carr and J. E. E. Baglin, At. Data Nucl. Data Tables **A10**, 143 (1971); R. M. Lazewski and R. J. Holt, *ibid.* **19**, 305 (1977).
[32]M. E. Rose, Phys. Rev. **91**, 610 (1953).
[33]D. W. Marquadt, J. Soc. Ind. Appl. Math. **11**, 431 (1963).
[34]W. J. O'Connell and S. S. Hanna, Phys. Rev. C **17**, 892 (1978).
[35]D. G. Mavis, Ph.D. thesis, Stanford University, 1977.
[36]J. R. Calarco, S. W. Wissink, M. Sasao, K. Wienhard, and S. S. Hanna, Phys. Rev. Lett. **39**, 925 (1977).
[37]S. W. Wissink, Ph.D. thesis, Stanford University, 1986.
[38]V. Gillet and N. Vinh-Mau, Nucl. Phys. **54**, 321 (1964).
[39]A. Arima and D. Strottman, Phys. Lett. **96B**, 23 (1980).
[40]K. A. Snover, E. G. Adelberger, P. G. Ikossi, and B. A. Brown, Phys. Rev. C **27**, 1837 (1983).
[41]G. Küchler, A. Richter, E. Spamer, W. Steffen, and W. Knüpfer, Nucl. Phys. **A406**, 473 (1983).
[42]C. Rolfs (private communication).
[43]C. W. DeJager, L. H. DeVries, and L. C. DeVries, At. Data Nucl. Data Tables **14**, 479 (1974).
[44]S. W. Wissink, J. R. Calarco, and S. S. Hanna, Nuclear Physics Laboratory, Stanford University, 1977–1979 Progress Report, 1979, p. 8.
[45]K. A. Snover, P. G. Ikossi, and T. A. Trainor, Phys. Rev. Lett. **43**, 117 (1979).
[46]C. Djalali, G. M. Crawley, B. A. Brown, V. Rotberg, G. Caskey, A. Galonsky, N. Marty, M. Morlet, and A. Willis, Phys. Rev. C **35**, 1201 (1987).